COMPARISON OF THE FRACTURE BEHAVIOUR OF A STRUCTURAL COMPONENT WITH TEST SPECIMEN BEHAVIOUR

B. K. Neale*

The rationale behind fracture toughness test procedures is discussed in terms of specimen data and areas are identified where further information is desirable. Application of specimen data to structural assessments is also considered.

Conservatisms implicit in testing and assessment procedures are examined by comparing fracture properties measured in a flawed structural componenet with results measured from test specimens.

INTRODUCTION

The main objective of fracture toughness testing procedures such as ASTM Standard 1152-87 (1), CEGB Procedure, Neale et al (2), and the EGF Procedure, Schwalbe et al (3), is to measure the fracture properties of a material using parameters which relate to structural behaviour. For ductile materials, the fracture parameters, which are usually based on either the J-integral or crack opening displacement, δ, are measured as a function of crack growth Δa.

The J-Δa behaviour of ferritic steels is known to vary with test specimen size and geometry. Testing procedures use bend type specimens which tend to exhibit lower bound data (4) compared with tensile specimens, Figure 1. The variation with test specimen size is unimportant if the thickness of the specimen is the same as the structural component and the crack orientation can be correctly modelled. Size effects are also relatively unimportant if the data are only used to compare the fracture properties of various steels for material selection purposes. However, size effects are important

* Central Electricity Generating Board, Berkeley Nuclear Laboratories, Berkeley, Glos. UK, GL13 9PB.

if the specimen size is less than the structural component as is often the case in the nuclear industry. In such situations, testing procedures apply validity limits, which are a function of specimen thickness, remaining ligament, crack growth and tensile properties. These limits are applied to specimen data to ensure that J and δ characterise the stress and strain fields ahead of the crack. Data of Ingham et al (5) shown in Figure 2 suggests the limits may be too restrictive. For example, the crack growth limit for the 20 mm compact tension specimens is nominally 1 mm whereas the data are essentially the same as those from larger specimens, at least up to 3 mm crack growth. Unfortunately such data cannot be generalised to other materials and without analytical or numerical justification the currently accepted validity limits cannot be reduced. Detailed finite element analyses of test specimens are currently being performed in the CEGB (6) and elsewhere to investigate validity limits. Experimental data in support of validity limits for δ are not as widespread as data for J so that, in addition to analytical or numerical analyses, considerably more experimental evidence is desirable in this case.

Testing procedures recommend the use of side grooved test specimens. Side grooving inhibits thumb-nailed crack growth and promotes straight fronted crack growth by enhancing the plane strain region ahead of the crack (7). Straight fronted crack growth removes any ambiguities in crack growth measurements and improves the accuracy of single specimen methods such as the unloading compliance technique. Increasing the plane strain region is equivalent to testing larger specimens. Figure 3 shows that the slope of the J-Δa curve decreases with increasing side groove depth which could be taken to imply a size dependence of J-Δa curves. This result is inconsistent with data shown in Figure 2 but is consistent with data of Roos (9), Figure 4. However, without testing large numbers of specimens, it is difficult to separate size effects from material scatter. For structural integrity assessments, application of the appropriate crack growth limits safeguards against non-conservatism in specimen data. Further work is required to assess the effect of side grooving and specimen size on the J-Δa curve.

Almost all of the methods used in testing procedures have been based on experience gained with ferritic steels and to a lesser extent aluminium alloys. To generalise the procedures further, a wider range of materials should be investigated. Austenitic steels are of interest to the nuclear and petro-chemical industries. In the aged

condition, austenitic steel can exhibit a wide range of material behaviour. At the extremes of behaviour it is difficult to generate valid data using existing test procedures. Preliminary results, Havel et al (10), indicated the absence of significant size and geometry effects between pre-cracked standard Charpy specimens and 25 mm compact tension specimens for a range of ageing conditions, Figure 5.

Assessment procedures

The integrity of defective structural components can be assessed using the R6 procedure, Milne et al (11), and J estimation techniques such as Kumar et al (12). An essential requirement of assessment procedures is knowledge of the fracture properties of the component steels. These properties should be demonstrably conservative and testing procedures recommend the use of bend specimens and side grooving. Overall conservatisms in assessment procedures can be estimated by comparing experimental failure loads with predictions. However, it is difficult to quantify whether any conservatism is arising in the assessment procedure or the fracture properties. The conservatism can be assessed by measuring the fracture resistance exhibited by a structural component and comparing the results with test specimen data. Unfortunately, there are few such comparisons available. Data are more commonly available comparing large scale specimens of approximately the same size as structural components, Figures 2 and 4, with test specimen data.

Comparison of specimens and structural behaviour

Angelino et al (13) have measurd the J-Δa behaviour of an axial through wall crack in a pressurised pipe and compared the results with data measured from similar thickness, non-side grooved compact tension specimens, Figure 6. They found the test specimen data were non-conservative compared with pipe results. On the other hand, Aerbeli et al (14), who performed similar tests, found virtually identical behaviour between pipe and test specimen data basing their comparison on crack opening displacements, Figure 7.

It was decided to examine the axial throughwall crack in a pressurised pipe further and the remainder of this paper describes tests similar to those performed by Angelino et al (13) and Aerbeli et al (14). The paper also compares the experimental results with elastic-plastic three-dimensional finite element analyses, Miller and Neale (15) in order to validate the test technique and assess the accurracy of the numerical results.

TEST DETAIL

Pipes were prepared with an external diameter of 100 mm, length of 450 mm and wall thickness of 5 mm from oversized pipe conforming to BS3602 steel. The machining required was sufficient to control tolerances on ovality, concentricity and parallelism.

Axial through wall cracks were spark eroded in the pipes to give crack lengths of 45, 50, 55 and 60 mm. The width of the cracks was nominally 0.30 mm.

The test rig consists of a pipe specimen enclosed by an outer perspex water containment vessel with associated pressurising and volume change measuring equipment, Figure 8. The external volume change was measured on a manometer from the water displaced as the pipe expands with pressurisation.

The accuracy of the testing configuration can be assessed by comparing the pressure volume change response of an uncracked pipe with an analytical approximation. In the elastic regime a measured response of 3.19 TPa m^{-3} was obtained. The Lamé solution relating the pressure P to the volume change V at the outer surface of the pipe is

$$\frac{P}{V} = \frac{E(b^2-a^2)}{\pi a^2 b^2 \ell(5-4\nu)} \qquad (1)$$

where a and b are the internal and external radii of the pipe respectively. It is difficult to give a precise value for the pipe length ℓ because of the change in throughwall thickness at the weldments and the effect of the end caps, connector ring and flanges of the test rig. However, it is greater than the gauge length of 0.42 m and less than the total length of 0.59 m. Assuming Young's modulus E of 204GPA, Poisson's ratio ν of 0.3, a of 0.045m, b of 0.050, then equation (1) predicts a slope between 3.82 and 2.71 TPa m^{-3} for ℓ of 0.42 and 0.59m, respectively. The measured response is within this range and the testing configuration is therefore considered accurate.

TEST METHOD

The J-Δa behaviour of the axial throughwall crack in a pressurised pipe was measured using the multiple specimen method similar to that descibed by Angelino et al (13) and Milella (16). The method involves measuring the pressure versus volume change of nominally identical pipes containing a range of crack lengths. From these data, a calibration function is derived for the fracture

resistance J as a function of volume change and pressure. A number of pipes containing the same initial crack length are then tested to different volume change levels to produce the pipe J, obtained from the calibration function, versus Δa, measured on the fracture surfaces, behaviour.

RESULTS

The experimentally derived J versus volume change and J versus pressure functions for a 50 mm throughwall axial crack in a pressurised pipe are show in Figures 9a and 9b, respectively. Details of the derivation are given in Neale and Haines (17). These functions are compared with three-dimensional finite element results, Miller and Neale (15), of the pipe obtained using the ABAQUS suite of programmes. There is reasonably good agreement between the experimental and numerical results. The element stiffness matrices were evaluated for both full and reduced integration. Reduced integration is believed to give more accurate results without the need for further mesh refinement. Any difference between full and reduced integration tends to suggest further mesh refinement is required. The full integration results are virtually the same as the experimental J versus pressure curve. For J versus volume change, the full and reduced integretion results are indistinquishable.

Figure 10 shows the J-Δa results of the multiple pipe tests. These results are compared with data obtained from pre-cracked Charpy specimens of nominally 6, 7 and 7.5 mm thickness tested in three-point bend, Neale (18), according to the CEGB Procedure (2). With the exception of one data point, the pipe results are within the scatterband of the Charpy specimen data. The exception at the lowest crack growth is probably due to crack tip root radius effects which may be suppressing crack initiation. Although more pipe results will be obtained, it does appear that there is no significant difference between pipe and specimen fracture behaviour.

In all cases thumb nailed crack growth occurred in the pipes more or less equally from both crack tips with the maximum extension tending towards the inner surface of the pipe.

CONCLUDING REMARKS

This paper has discussed the rationale behind testing procedures and identified areas where further investigation is required. The implications for structural integrity assessments which make use of such

data have been discussed in terms of published work and tests performed on a throughwall axial crack in a pressurised pipe. The fracture resistance measured on the pipe tests described here was virtually the same as that obtained from non-side grooved, pre-cracked Charpy specimens. This implies that for this geoemtry, testing procedures provide accurate fracture data for assessment purposes.

The use of finite element methods for assessments has been examined by calculating J as a function of pressure and volume change. The calculated J functions have been found to be in reasonable agreement with the experimentally measured functions, indicating that finite element methods in conjunction with test specimen data would accurately predict pipe behaviour.

The use of approximate assessment techniques such as R6 (11) can also be examined for the pipe results. The material specific failure assessment curve was derived for the pipe using the stress-strain curve of the steel. All the pipe results lie outside the assessment curve, Figure 11. As the test specimen data are known to accurately represent the pipe behaviour, this means that for the pipe geomtry there is conservatism in the failure assessment curve.

ACKNOWLEDGEMENT

This work was carried out at the Berkeley Nuclear Laboratories of the Technology, Planning and Research Division and the paper is published by permission of the Central Electricity Generating Board.

SYMBOLS USED

a, b = internal and external radii of pipe

E = Young's modulus

J = fracture resistance

K_r, L_r = R6 assessment parameters

ℓ = effective pipe length

P = pressure

V = volume change

δ = crack tip opening displacement

Δa = crack growth

ν = Poisson's ratio

REFERENCES

(1) Annual Book of ASTM Standards, E1152-87, Vol. 03.01, 1987.

(2) Neale, B.K., Curry, D.A., Green, G., Haigh, J.R. and Akhurst, K.N., Int. J. of Pressure Vessels and Piping, 20 (3), 1985, pp. 157-179.

(3) Schwalbe, K.H., Neale, B.K. and Ingham, T., "The development of a European Group on Fracture procedure to measure elastic-plastic fracture parameters", Proc. of the 6th European Conference on Fracture, Amsterdam, 1986, pp. 277-299.

(4) Garwood, S.J., "Crack growth resistance-geoemtry effects and structural predictions in A533B class 1 steel", CSNI Specialists' Meeting on Plastic Tearing Instability, St. Louis, Missouri, 1979, pp. 226-269.

(5) Ingham, T., Bland, J.T. and Wardle, G., "The influence of specimen size on the upper shelf toughness of A533B-1 steel", 7th Int. Conf. on Structural Mechanics in Reactor Technology, G2/3, Chicago, Illinois, 1983.

(6) Goldthorpe, M.R., "A finite element investigation of the effect of specimen geometry on crack tip fields in hardening materials", CEGB Report OED/STN/87/20185/R, 1987.

(7) Neale, B.K., Int. J. of Pressure Vessels and Piping, 10(5), 1982, pp. 375-398.

(8) Vassilaros, M.G., Joyce, J.A. and Gudas, J.P., ASTM STP 700, 1980, pp. 251-270.

(9) Roos, E., "Component tests and R-curve approach for through cracks", Advanced Seminar on Fracture Mechanics (ASFM6), Ispra, 1987.

(10) Havel, R., Neale, B.K. and Senior, B.A., "The fracture properties of aged 316 austenitic steel", CEGB Report TPRD/B/0914/R87, 1987.

(11) Milne, I., Ainsworth, R.A., Dowling, A.R. and Stewart, A.T., "Assessment of the integrity of structures containing defects", CEGB Report R/H/R6 - Revision 3, 1986.

(12) Kumar, V., German, M.D. and Shih, C.F., "An engineering approach for elastic-plastic fracture", EPRI report NP 1931, 1981.

(13) Angelino, G., Squilloni, S. and Reale, S., "Experimental application of EPFM to through thickness cracked pipes", Proc. of a CSNI Workshop on Ductile Fracture Test Methods, Paris, 1983, pp. 323-329.

(14) Aerbeli, K.E., Schulze, D., Morawietz, P., Fuhlrott, H., Heerens, J. and Schwalbe, K - H., "Fracture mechanics tests on axially cracked pipe sections subjected to internal pressure", GKSS Report 85/E/62, 1986.

(15) Miller, A.G. and Neale, B.K., "The fracture behaviour of an axial crack in a pressurised pipe- numerical analysis", CEGB Report TPRD/B/0987/R87, 1988.

(16) Milella, P.P., Nuclear Engng. and Design, 98, 1987, pp. 219-229.

(17) Neale, B.K. and Haines, A.B., "The fracture behaviour of an axial crack in a pressurised pipe - experimental investigation", CEGB Report in preparation.

(18) Neale, B.K., "The fracture behaviour of an axial crack in a pressurised pipe - material characterisation", CEGB Report TPRD/B/0936/R87, 1987.

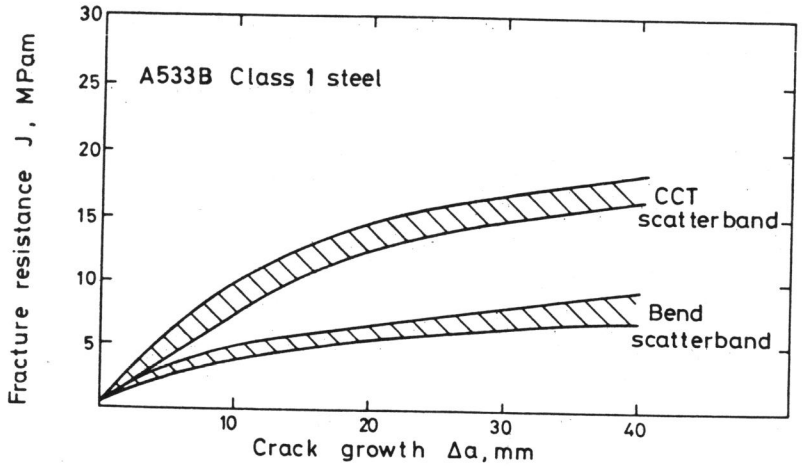

Figure 1 Comparison of bend and tensile specimen behaviour, Garwood (4)

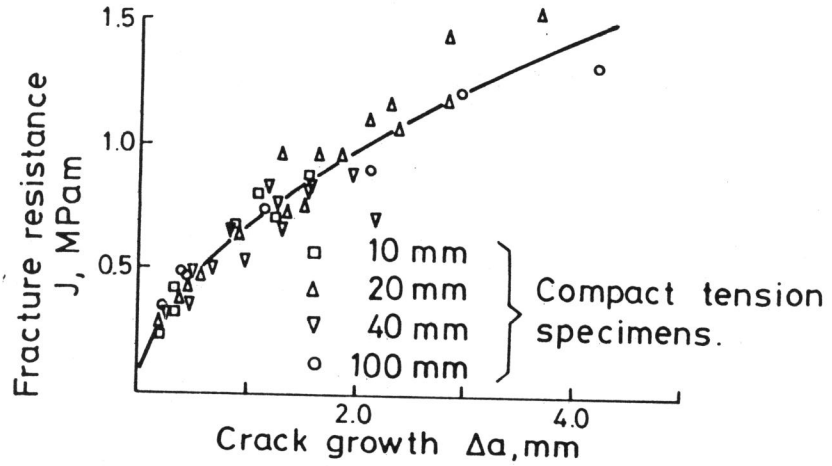

Figure 2 J-Δa behaviour of A533B Class 1 steel, Ingham et al (5)

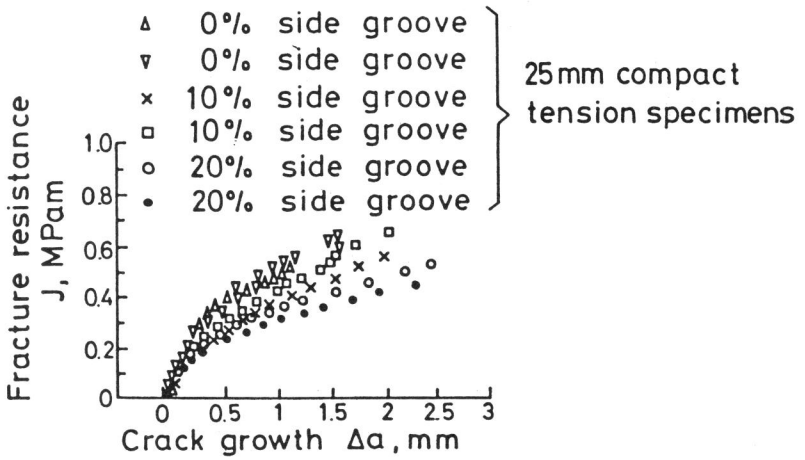

Figure 3 J-Δa behaviour of A533B steel, Vassilaros et al (8)

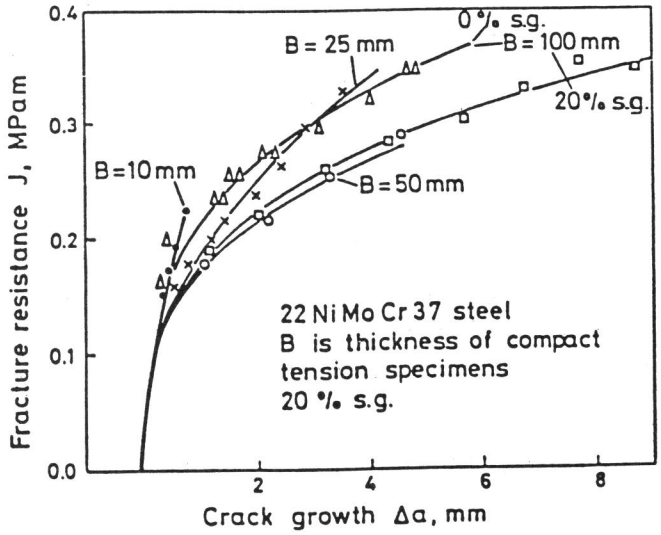

Figure 4 Effect of specimen size and side grooving on J-Δa data, Roos (9)

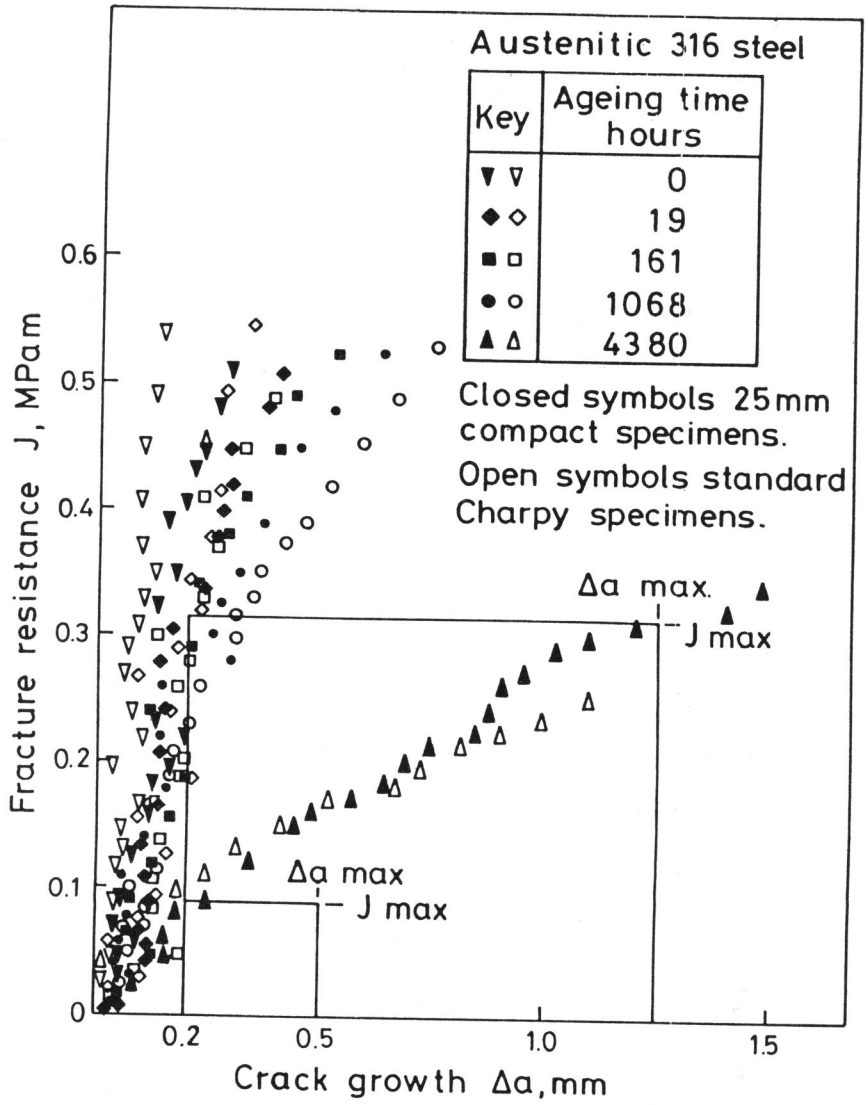

Figure 5 Comparison of Charpy and compact specimen J-Δa data, Havel et al (10)

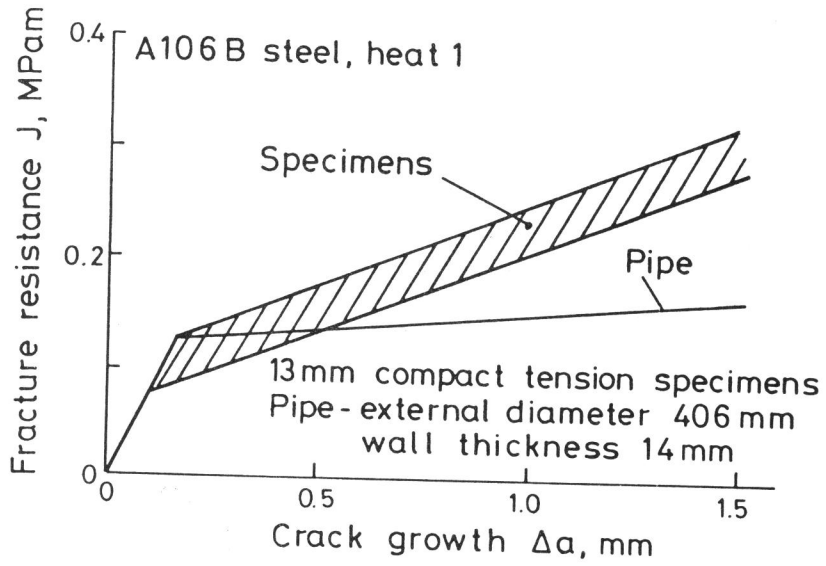

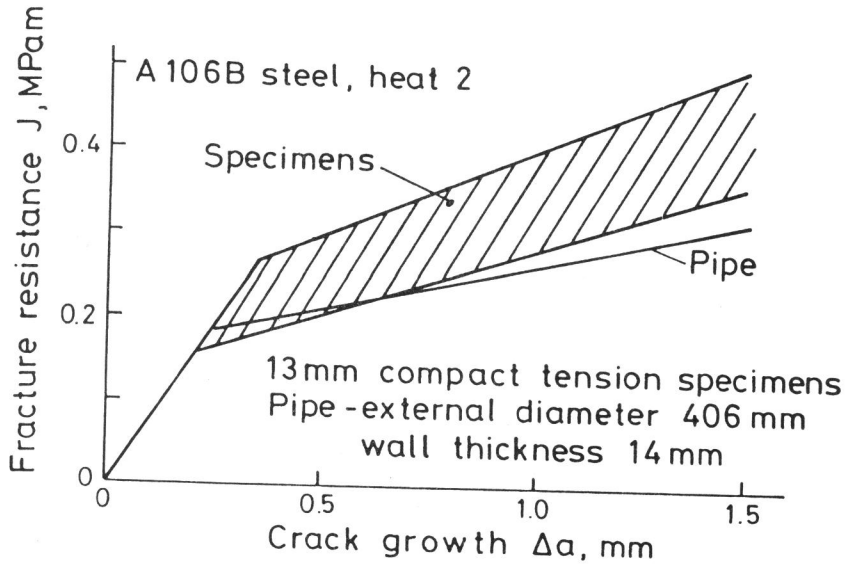

Figure 6 Comparison between specimen and pipe results, Angelino et al (13)

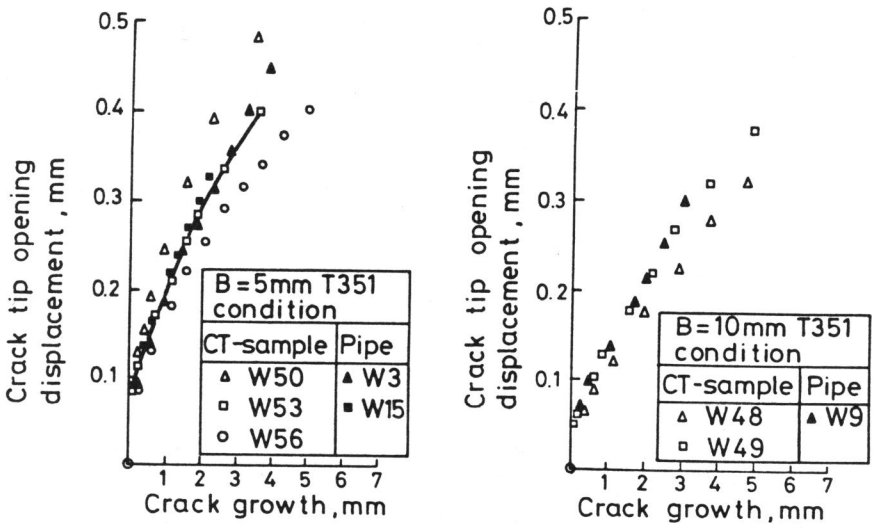

Figure 7 Comparison between specimen and pipe results, Aerbeli et al (14)

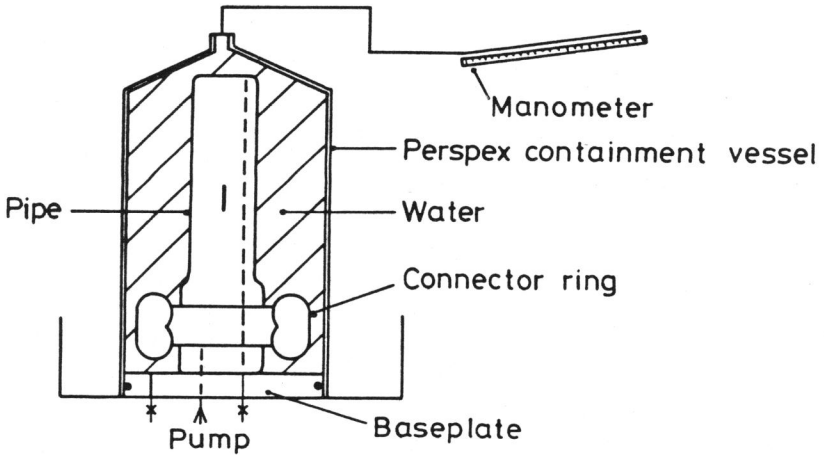

Figure 8 Schematic of test configuration

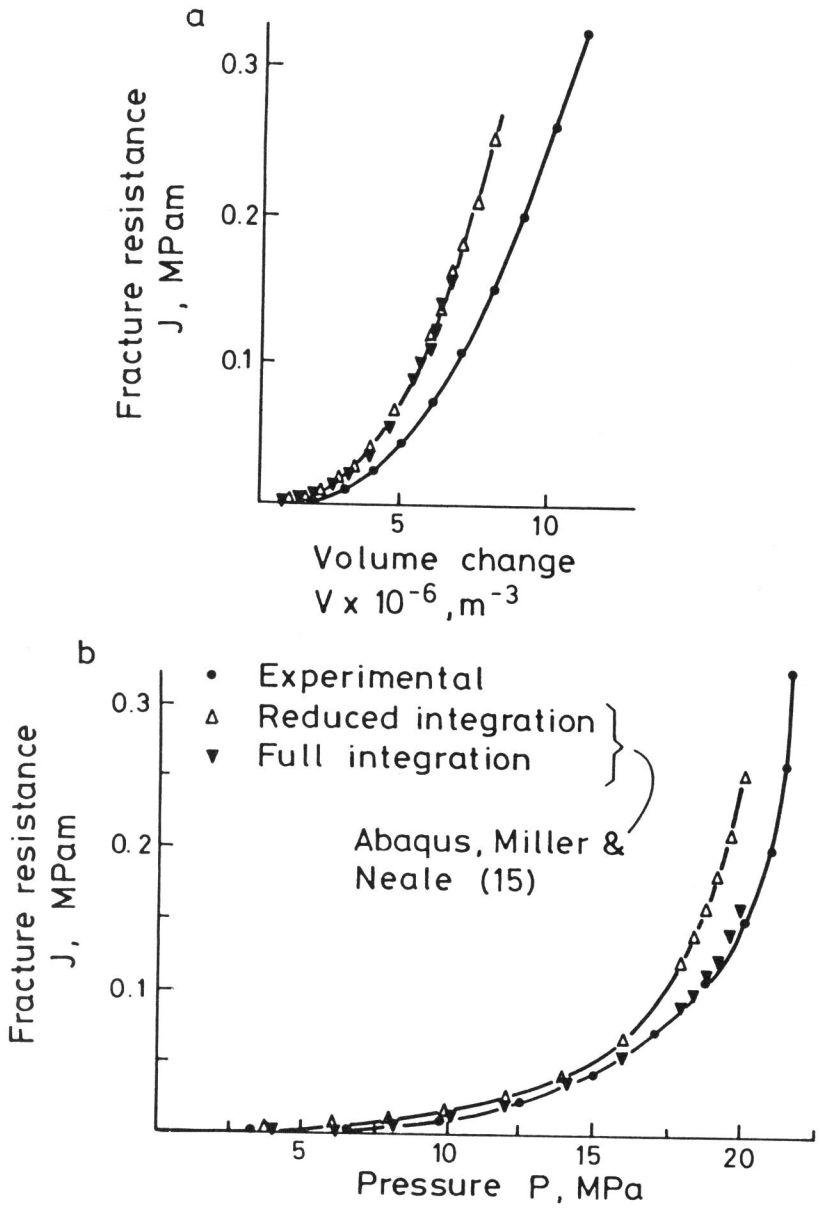

Figure 9 J calibration functions compared with finite element results

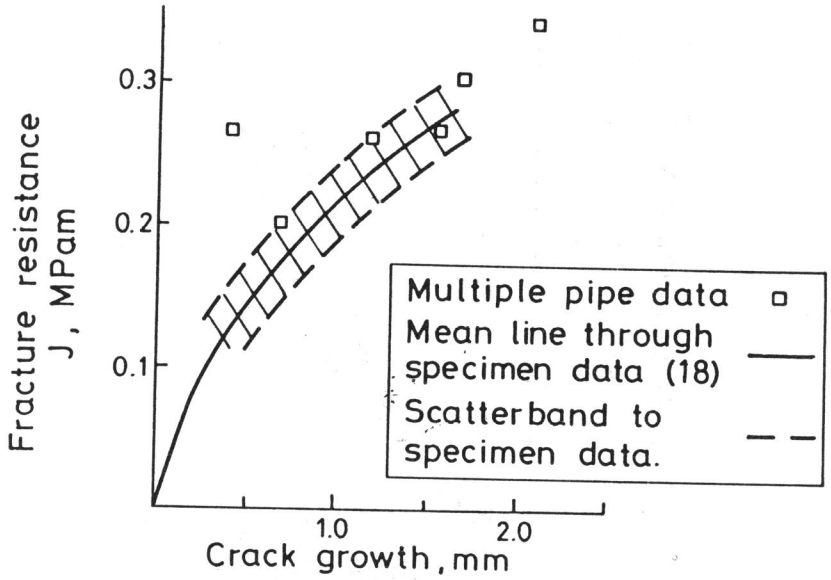

Figure 10 Comparison between specimen and pipe results, Neale and Haines (17)

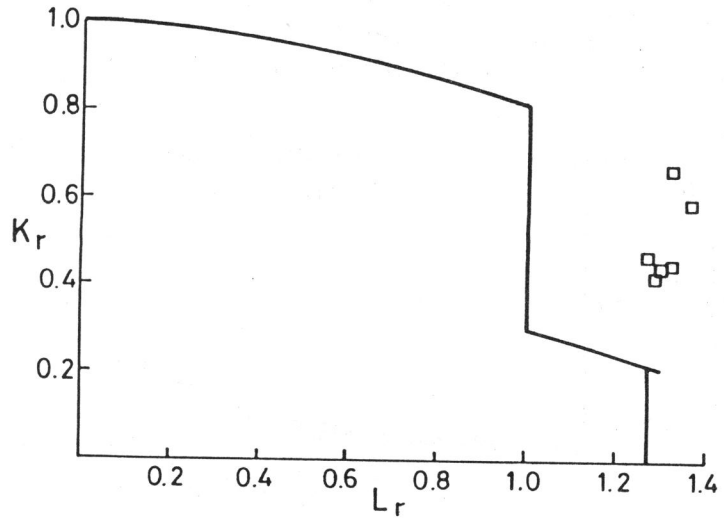

Figure 11 R6 assessment of pipe data